Nanomaterials Chemistry

Recent Developments and New Directions

Edited by
C. N. R. Rao, A. Müller, and A. K. Cheetham

WILEY-VCH Verlag GmbH & Co. KGaA

Nanomaterials Chemistry

Edited by
C. N. R. Rao, A. Müller,
and A. K. Cheetham

1807–2007 Knowledge for Generations

Each generation has its unique needs and aspirations. When Charles Wiley first opened his small printing shop in lower Manhattan in 1807, it was a generation of boundless potential searching for an identity. And we were there, helping to define a new American literary tradition. Over half a century later, in the midst of the Second Industrial Revolution, it was a generation focused on building the future. Once again, we were there, supplying the critical scientific, technical, and engineering knowledge that helped frame the world. Throughout the 20th Century, and into the new millennium, nations began to reach out beyond their own borders and a new international community was born. Wiley was there, expanding its operations around the world to enable a global exchange of ideas, opinions, and know-how.

For 200 years, Wiley has been an integral part of each generation's journey, enabling the flow of information and understanding necessary to meet their needs and fulfill their aspirations. Today, bold new technologies are changing the way we live and learn. Wiley will be there, providing you the must-have knowledge you need to imagine new worlds, new possibilities, and new opportunities.

Generations come and go, but you can always count on Wiley to provide you the knowledge you need, when and where you need it!

William J. Pesce
President and Chief Executive Officer

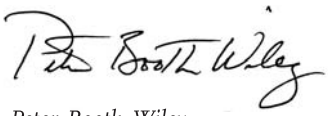

Peter Booth Wiley
Chairman of the Board

Nanomaterials Chemistry

Recent Developments and New Directions

Edited by
C. N. R. Rao, A. Müller, and A. K. Cheetham

WILEY-VCH Verlag GmbH & Co. KGaA

The Editors

Prof. Dr. C. N. R. Rao
Jawaharlal Nehru Centre for Advanced Scientific Research
CSIR Centre of Excellence in Chemistry and Chemistry and Physics of Materials Unit
Jakkur P.O.
Bangalore 560 064
India

Prof. Dr. Dr. h.c. mult. A. Müller
University of Bielefeld
Faculty of Chemistry
P. O. Box 10 01 31
33501 Bielefeld
Germany

Prof. Dr. A. K. Cheetham
University of California
Materials Research Laboratory
Santa Barbara, CA 93106-5130
USA

Library of Congress Card No.: applied for

British Library Cataloguing-in-Publication Data
A catalogue record for this book is available from the British Library.

Bibliographic information published by the Deutsche Nationalbibliothek
Die Deutsche Nationalbibliothek lists this publication in the Deutsche National-bibliografie; detailed bibliographic data are available in the Internet at ⟨http://dnb.d-nb.de⟩.

Printed in the Federal Republic of Germany
Printed on acid-free paper

Typesetting Asco Typesetter, Hong Kong
Printing betz-druck GmbH, Darmstadt
Binding Litges & Dopf GmbH, Heppenheim
Wiley Bicentennial Logo Richard J. Pacifico

ISBN 978-3-527-31664-9

Contents

Preface *XI*

List of Contributors *XIII*

1 Recent Developments in the Synthesis, Properties and Assemblies of Nanocrystals *1*
P.J. Thomas and P. O'Brien

1.1 Introduction *1*
1.2 Spherical Nanocrystals *1*
1.2.1 Semiconductor Nanocrystals *1*
1.2.2 Metal Nanocrystals *4*
1.2.3 Nanocrystals of Metal Oxides *6*
1.3 Nanocrystals of Different Shapes *7*
1.3.1 Anisotropic Growth of Semiconductor and Oxide Nanocrystals *7*
1.3.2 Anisotropic Growth of Metal Nanocrystals *14*
1.4 Selective Growth on Nanocrystals *17*
1.5 Properties of Nanocrystals *18*
1.5.1 Electronic and Optical Properties *18*
1.5.2 Magnetic Properties *21*
1.6 Ordered Assemblies of Nanocrystals *22*
1.6.1 One- and Low-dimensional Arrangements *22*
1.6.2 Two-dimensional Arrays *24*
1.6.3 Three-dimensional Superlattices *26*
1.6.4 Colloidal Crystals *29*
1.7 Applications *30*
1.7.1 Optical and Electro-optical Devices *30*
1.7.2 Nanocrystal-based Optical Detection and Related Devices *31*
1.7.3 Nanocrystals as Fluorescent Tags *33*
1.7.4 Biomedical Applications of Oxide Nanoparticles *33*
1.7.5 Nanoelectronics and Nanoscalar Electronic Devices *34*
1.8 Conclusions *35*
References *36*

2 Nanotubes and Nanowires: Recent Developments *45*
S. R. C. Vivekchand, A. Govindaraj, and C. N. R. Rao

2.1 Introduction *45*
2.2 Carbon Nanotubes *45*
2.2.1 Synthesis *45*
2.2.2 Purification *50*
2.2.3 Functionalization and Solubilization *54*
2.2.4 Properties and Applications *60*
2.2.4.1 Optical, Electrical and Other Properties *60*
2.2.4.2 Phase Transitions, Mechanical Properties, and Fluid Mechanics *66*
2.2.4.3 Energy Storage and Conversion *68*
2.2.4.4 Chemical Sensors *68*
2.2.5 Biochemical and Biomedical Aspects *69*
2.2.6 Nanocomposites *71*
2.2.7 Transistors and Devices *72*
2.3 Inorganic Nanotubes *75*
2.3.1 Synthesis *75*
2.3.2 Solubilization and Functionalization *77*
2.3.3 Properties and Applications *79*
2.4 Inorganic Nanowires *79*
2.4.1 Synthesis *79*
2.4.2 Self Assembly and Functionalization *90*
2.4.3 Coaxial Nanowires and Coatings on Nanowires *92*
2.4.4 Optical Properties *92*
2.4.5 Electrical and Magnetic Properties *97*
2.4.6 Some Chemical Aspects and Sensor Applications *100*
2.4.7 Mechanical Properties *101*
2.4.8 Transistors and Devices *102*
2.4.9 Biological Aspects *103*
References *104*

3 Nonaqueous Sol–Gel Routes to Nanocrystalline Metal Oxides *119*
M. Niederberger and M. Antonietti

3.1 Overview *119*
3.2 Introduction *119*
3.3 Short Introduction to Aqueous and Nonaqueous Sol–Gel Chemistry *120*
3.4 Nonaqueous Sol–Gel Routes to Metal Oxide Nanoparticles *121*
3.4.1 Surfactant-controlled Synthesis of Metal Oxide Nanoparticles *121*
3.5 Solvent-controlled Synthesis of Metal Oxide Nanoparticles *127*
3.5.1 Introduction *127*
3.5.2 Reaction of Metal Halides with Alcohols *127*
3.5.3 Reaction of Metal Alkoxides with Alcohols *130*
3.5.4 Reaction of Metal Alkoxides with Ketones and Aldehydes *131*

3.5.5 Reaction of Metal Acetylacetonates with Various Organic Solvents *132*
3.6 Selected Reaction Mechanisms *133*
3.7 Summary and Outlook *134*
References *135*

4 Growth of Nanocrystals in Solution *139*
R. Viswanatha and D.D. Sarma

4.1 Introduction *139*
4.2 Theoretical Aspects *140*
4.2.1 Theory of Nucleation *140*
4.2.2 Mechanism of Growth *141*
4.2.2.1 Diffusion Limited Growth: Lifshitz–Slyozov–Wagner (LSW) Theory and Post-LSW Theory *143*
4.2.2.2 Reaction-limited Growth *147*
4.2.2.3 Mixed Diffusion–Reaction Control *148*
4.3 Experimental Investigations *151*
4.3.1 Au Nanocrystals *153*
4.3.2 ZnO Nanocrystals *154*
4.3.3 Effect of Capping Agents on Growth Kinetics *160*
4.3.3.1 Effect of Oleic Acid on the Growth of CdSe Nanocrystals *161*
4.3.3.2 PVP as a Capping Agent in the Growth of ZnO Nanocrystals *163*
4.3.3.3 Effect of Adsorption of Thiols on ZnO Growth Kinetics *166*
4.4 Concluding Remarks *167*
References *168*

5 Peptide Nanomaterials: Self-assembling Peptides as Building Blocks for Novel Materials *171*
M. Reches and E. Gazit

5.1 Overview *171*
5.2 Introduction *171*
5.3 Cyclic Peptide-based Nanostructures *172*
5.4 Linear Peptide-based Nanostructures *174*
5.5 Amyloid Fibrils as Bio-inspired Material: The Use of Natural Amyloid and Peptide Fragments *177*
5.6 From Amyloid Structures to Peptide Nanostructures *178*
5.7 Bioinspired Peptide-based Composite Nanomaterials *180*
5.8 Prospects *180*
References *181*

6 Surface Plasmon Resonances in Nanostructured Materials *185*
K.G. Thomas

6.1 Introduction to Surface Plasmons *185*
6.1.1 Propagating Surface Plasmons *186*

6.1.2 Localized Surface Plasmons *189*
6.2 Tuning the Surface Plasmon Oscillations *190*
6.2.1 Size of Nanoparticle *190*
6.2.2 Shape of Nanoparticle *191*
6.2.3 Dielectric Environment *194*
6.3 Excitation of Localized Surface Plasmons *196*
6.3.1 Multipole Resonances *197*
6.3.2 Absorption vs. Scattering *200*
6.4 Plasmon Coupling in Higher Order Nanostructures *204*
6.4.1 Assembly of Nanospheres *204*
6.4.2 Assembly of Nanorods *208*
6.5 Summary and Outlook *215*
References *216*

7 Applications of Nanostructured Hybrid Materials for Supercapacitors *219*
A.V. Murugan and K. Vijayamohanan

7.1 Overview *219*
7.2 Introduction *219*
7.3 Nanostructured Hybrid Materials *220*
7.4 Electrochemical Energy Storage *222*
7.5 Electrochemical Capacitors *223*
7.5.1 Electrochemical Double Layer Capacitor vs. Conventional Capacitor *225*
7.5.2 Origin of Enhanced Capacitance *226*
7.6 Electrode Materials for Supercapacitors *229*
7.6.1 Nanostructured Transition Metal Oxides *229*
7.6.2 Nanostructured Conducting Polymers *230*
7.6.3 Carbon Nanotubes and Related Carbonaceous Materials *231*
7.7 Hybrid Nanostructured Materials *234*
7.7.1 Conducting Polymer–Transition Metal Oxide Nanohybrids *235*
7.7.2 Conducting Polymer–Carbon Nanotube Hybrids *237*
7.7.3 Transition Metal Oxides–Carbon Nanotube Hybrids *238*
7.8 Hybrid Nanostructured Materials as Electrolytes for Super Capacitors *241*
7.8.1 Nanostructured Polymer Composite Electrolytes *242*
7.8.2 Ionic Liquids as Supercapacitor Electrolytes *242*
7.9 Possible Limitations of Hybrid Materials for Supercapacitors *243*
7.10 Conclusions and Perspectives *244*
References *245*

8 Dendrimers and Their Use as Nanoscale Sensors *249*
N. Jayaraman

8.1 Introduction *249*
8.2 Synthetic Methods *250*
8.3 Macromolecular Properties *262*

8.3.1 Molecular Modeling and Intrinsic Viscosity Studies *262*
8.3.2 Fluorescence Properties *264*
8.3.3 *Endo*- and *Exo*-Receptor Properties *265*
8.4 Chemical Sensors with Dendrimers *267*
8.4.1 Vapor Sensing *267*
8.4.2 Sensing Organic Amines and Acids *270*
8.4.3 Vapoconductivity *270*
8.4.4 Sensing CO and CO_2 *271*
8.4.5 Gas and Vapor Sensing in Solution *272*
8.4.6 Chiral Sensing of Asymmetric Molecules *275*
8.4.7 Fluorescence Labeled Dendrimers and Detection of Metal Cations *277*
8.4.8 Anion Sensing *279*
8.5 Dendrimer-based Biosensors *281*
8.5.1 Acetylcholinesterase Biosensor *281*
8.5.2 Dendrimers as Cell Capture Agents *282*
8.5.3 Dendrimers as a Surface Plasmon Resonance Sensor Surface *283*
8.5.4 Layer-by-Layer Assembly Using Dendrimers and Electrocatalysis *283*
8.5.5 SAM–Dendrimer Conjugates for Biomolecular Sensing *284*
8.5.6 Dendrimer-based Calorimetric Biosensors *288*
8.5.7 Dendrimer-based Glucose Sensors *289*
8.6 Conclusion and Outlook *292*
References *292*

9 Molecular Approaches in Organic/Polymeric Field-effect Transistors *299*
K. S. Narayan and S. Dutta

9.1 Introduction *299*
9.2 Device Operations and Electrical Characterization *300*
9.3 Device Fabrication *301*
9.3.1 Substrate Treatment Methods *304*
9.3.2 Electrode Materials *305*
9.4 Progress in Electrical Performance *306*
9.5 Progress in p-Channel OFETs *306*
9.6 Progress in n-Channel OFET *309*
9.7 Progress in Ambipolar OFET *310*
9.8 PhotoPFETs *311*
9.9 Photoeffects in Semiconducting Polymer Dispersed Single Wall Carbon Nanotube Transistors *313*
9.10 Recent Approaches in Assembling Devices *314*
References *316*

10 Supramolecular Approaches to Molecular Machines *319*
M. C. Grossel

10.1 Introduction *319*
10.2 Catenanes and Rotaxanes *320*
10.2.1 Synthetic Routes to Catenanes and Rotaxanes *321*

10.2.2 Aromatic π–π Association Routes to Catenanes and Rotaxanes *322*
10.2.2.1 Preparation and Properties of [2]-Catenanes *322*
10.2.2.2 Multiple Catenanes *323*
10.2.2.3 Switchable Catenanes *324*
10.2.2.4 Other Synthetic Routes to Paraquat-based Catenanes *326*
10.2.2.5 Rotaxane Synthesis *328*
10.2.2.6 Switchable Catenanes *328*
10.2.2.7 Neutral Catenane Assembly *329*
10.2.3 Ion Templating *329*
10.2.3.1 Approaches to Redox-switchable Catenanes and Rotaxanes *329*
10.2.3.2 Making More Complex Structures *332*
10.2.3.3 Routes to [n]-Rotaxanes using Olefin Metathesis – Molecular Barcoding *333*
10.2.3.4 Anion-templating *335*
10.2.3.5 Other Approaches to Ion-templating *337*
10.2.4 Hydrogen-bonded Assembly of Catenane, Rotaxanes, and Knots *338*
10.2.4.1 Catenane and Knotane Synthesis *338*
10.2.4.2 Routes to Functional Catenanes and Rotaxanes *339*
10.2.4.3 Catenanes and Rotaxanes Derived from Dialkyl Ammonium Salts *346*
10.2.5 Cyclodextrin-based Rotaxanes *348*
10.2.5.1 Controlling Motion *349*
10.3 Molecular Logic Gates *349*
10.4 Conclusions *352*
References *352*

11 Nanoscale Electronic Inhomogeneities in Complex Oxides *357*
V. B. Shenoy, H. R. Krishnamurthy, and T. V. Ramakrishnan

11.1 Introduction *357*
11.2 Electronic Inhomogeneities – Experimental Evidence *358*
11.3 Theoretical Approaches to Electronic Inhomogeneities *364*
11.4 The ℓb Model for Manganites *366*
11.5 The Extended ℓb Model and Effects of Long-range Coulomb Interactions *370*
11.6 Conclusion *381*
References *382*

Index *385*

Preface

The subject of nanoscience and technology has had an extraordinary season of development and excitement in the last few years. Chemistry constitutes a major part of nanoscience research and without employing chemical techniques it is difficult, nay impossible, to synthesize or assemble most of the nanomaterials. Furthermore, many of the properties and phenomena associated with nanomaterials require chemical understanding, just as many of the applications of nanomaterials relate to chemistry. Because of the wide interest in the subject, we edited a book entitled Chemistry of Nanomaterials, which was published by Wiley-VCH in the year 2004. This book was extremely well received. In view of the increasing interest evinced all over the world in the chemistry of nanomaterials, we considered it appropriate to edit a book covering research on nanomaterials published in the last 2 to 3 years. This book is the result of such an effort. The book covers recent developments in nanocrystals, nanotubes and nanowires. The first two chapters dealing with nanocrystals, nanotubes and nanowires broadly cover all aspects of these three classes of nanomaterials. There are also chapters devoted to topics such as peptide nanomaterials, dendrimers, molecular electronics, molecular motors and supercapacitors. We believe that this book not only gives a status report of the subject, but also indicates future directions. The book should be a useful guide and reference work to all those involved in teaching and research in this area.

C. N. R. Rao
A. Müller
A. K. Cheetham

List of Contributors

M. Antonietti
Max Planck Institute of Colloids and Interfaces
Colloid Chemistry
Research Campus Golm
14424 Potsdam
Germany

A.K. Cheetham
University of California
Materials Research Laboratory
Santa Barbara, CA 93106-5130
USA

S. Dutta
ISMN-CNR Bologna Division
Via P. Gobetti, 101
40129 Bologna
Italy

E. Gazit
Faculty of Life Sciences
Ramat Aviv
Tel Aviv Univeristy
Tel Aviv 69978
Israel

A. Govindaraj
Hon. Faculty Fellow
CSIR COE in Chemistry &
DST Unit on Nanoscience
JNCASR, Jakkur PO
Bangalore 560064
India

M.C. Grossel
School of Chemistry
University of Southampton
Highfield
Southampton
Hants
SO17 1BJ
UK

N. Jayaraman
Department of Organic Chemistry
Indian Institute of Science
Bangalore 560 012
India

H.R. Krishnamurthy
Centre for Condensed Matter Theory
Indian Institute of Science
Bangalore 560 012
India

A. Müller
University of Bielefeld
Faculty of Chemistry
P.O. Box 10 01 31
33501 Bielefeld
Germany

A.V. Murugan
Physical and Materials Chemistry Division
National Chemical Laboratory
Pune 411 008
India

K.S. Narayan
Jawaharlal Nehru Centre for
Advanced Scientific Research
Bangalore 560 064
India

M. Niederberger
Max Planck Institute of Colloids
and Interfaces
Colloid Chemistry
Research Campus Golm
14424 Potsdam
Germany

P. O'Brien
School of Chemistry and School
of Materials
The University of Manchester
Oxford Road
Manchester
M139PL
UK

T.V. Ramakrishnan
Department of Physics
Banaras Hindu University
Varanasi 221 005
Uttar Pradesh
India

C.N.R. Rao
Jawaharlal Nehru Centre for
Advanced Scientific Research
CSIR Centre of Excellence in
Chemistry and Chemistry and
Physics of Materials Unit
Jakkur P.O.
Bangalore 560 064
India

M. Reches
Department of Molecular
Microbiology and Biotechnology
Tel Aviv University
Tel Aviv 69978
Israel

D.D. Sarma
Solid State and Structural Chemistry
Unit
Indian Institute of Science
Bangalore 560 012
India

V.B. Shenoy
Materials Research Centre and Centre
for Condensed Matter Theory
Indian Institute of Science
Bangalore 560 012
India

K.G. Thomas
Photosciences and Photonics
Chemical Sciences and Technology
Division
Regional Research Laboratory
Trivandrum 695 019
India

P.J. Thomas
School of Chemistry and School of
Materials
The University of Manchester
Oxford Road
Manchester
M139PL
UK

K. Vijayamohanan
Physical and Materials Chemistry
Division
National Chemical Laboratory
Pune 411 008
India

R. Viswanatha
Solid State and Structural Chemistry
Unit
Indian Institute of Science
Bangalore 560 012
India

S.R.C. Vivekchand
Jawaharlal Nehru Centre for
Advanced Scientific Research
Chemistry and Physics of Materials
Unit and DST Unit on Nanoscience
Jakkur P. O.
Bangalore 560 064
India

1
Recent Developments in the Synthesis, Properties and Assemblies of Nanocrystals

P.J. Thomas and P. O'Brien

1.1
Introduction

Nanocrystals of metals, oxides and semiconductors have been studied intensely in the last several years by different chemical and physical methods. In the past decade the realization that the electronic, optical, magnetic and chemical properties of nanocrystals depend on their size has motivated intense research in this area. This interest has resulted in better understanding of the phenomena of quantum confinement, mature synthetic schemes and fabrication of exploratory nanoelectronic devices. The past couple of years has seen heightened activity in this area, driven by advances such as the ability to synthesize nanocrystals of different shapes. In this chapter, we review the progress in the area in the above period with emphasis on growth of semiconductor nanocrystals. Illustrative examples of the advances are provided. Several reviews have appeared in this period, seeking to summarize past as well as current work [1–4].

1.2
Spherical Nanocrystals

1.2.1
Semiconductor Nanocrystals

There have been several successful schemes for the synthesis of monodisperse semiconductor nanocrystals, especially the sufides and selenides of cadmium. However, there is still plenty of interest in exploring new synthetic routes. Nanocrystals of lead, manganese, cadmium and zinc sulfides have been obtained by thermolysis of the corresponding metal-oleylamine complex in the presence of S dissolved in oleylamine. The metal oleylamine complexes were prepared by reacting the corresponding chlorides with oleylamine. Nanocrystals with elongated shapes such as bullets and hexagons were produced by varying the stoichiometry

and concentration of the precursors [5]. Manganese sulfide nanocrystals in the form of spheres and other shapes such as wires and cubes have been obtained by thermolysis of the diethyldithiocarbamate in hexadecylamine [6]. Nanocrystals of cadmium, manganese, lead, copper and zinc sulphides have been obtained by thermal decomposition of hexadecylxanthates in hexadecylamine and other solvents. A highlight of this report is the use of relatively low temperatures (50–150 °C) and ambient conditions for synthesis of the nanocrystals [7]. Fluorescent CdSe nanocrystals have been prepared using the air stable single source precursor cadmium imino-bis(diisopropylphosphine selenide) [8]. Cadmium selenide nanocrystals have been prepared in an organic medium prepared without the use of phosphines or phosphine oxides using CdO in oleic acid and Se in octadecene [9]. Water soluble luminescent CdS nanocrystals have been prepared by refluxing a single source precursor [(2,2′-bipyridine)$Cd(SCOPh)_2$] in aqueous solution [10]. Nanocrystals of EuS exhibiting quantum confinement were synthesized for the very first time by irradiating a solution of the dithiocarbamate $Na[Eu(S_2CNEt_2)_4]3.5H_2O$ in acetonitrile [11]. Following this initial report, a number of single source precursors have been used to synthesize EuS nanocrystals [12].

Peng and coworkers have followed the nucleation and growth of CdSe nanocrystals in real time by monitoring absorption spectra with millisecond resolution [13]. Extremely small CdSe nanocrystals with dimensions of about 1.5 nm, with magic nuclearity have been reproducibly synthesized starting with CdO [14]. Intense emission, due to defects, spread across the visible spectrum has been observed from these nanocrystals (see Fig. 1.1). These nanocrystals can therefore be used to obtain white emission. The nanocrystals are presumed to have the structure of highly stable CdSe clusters observed in mass spectrometric studies [15].

Chalcogenide semiconductor nanocrystals have been synthesized in microfabricated flow reactors [16, 17]. The reactors employ either a continuous stream of

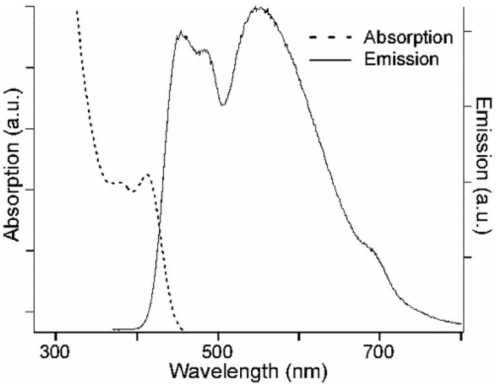

Fig. 1.1 Absorption and emission spectra of magic-sized CdSe nanocrystals (reproduced with permission from Ref. [14]).

liquid [16] or a segmented column containing gas and liquid droplets [17]. The use of small volumes and microscopic cells, provides new avenues for easy study of the nanocrystal growth process.

Gallium arsenide nanocrystals with diameters in the range 2.0–6.0 nm have been prepared in 4-ethylpyridine starting with $GaCl_3$ and $As(NMe_2)_3$ [18]. Highly luminescent InAs nanocrystals have been prepared in hexadecylamine by the use of the single source precursor $[^tBu_2AsInEt_2]_2$ [19].

Sardar and Rao [20] have prepared GaN nanoparticles of various sizes under solvothermal conditions, employing gallium cupferronate ($Ga(C_6H_5N_2O_2)_3$) or chloride ($GaCl_3$) as the gallium source and hexamethyldisilyzane as nitriding agent and toluene as solvent. This method is generally applicable for nitridation reactions. Nanocrystals of InP and GaP have been prepared using the thermolysis of the metal diorganophosphide $[M(P^tBu_2)_3]$ in hot 4-ethylpyridine [21], InP nanoparticles of different sizes (12–40 nm) have been prepared by a the solvothermal reaction involving $InCl_3$ and Na_3P [22]. Magnetic MnP nanocrystals with diameters of 6.7 nm have been produced by the treatment of $Mn_2(CO)_{10}$ with $P(SiMe_3)_3$ in trioctylphosphine oxide (TOPO)/myristic acid at elevated temperature [23]. Nanocrystals of iron and cobalt phosphides can also be synthesized by the use of the corresponding carbonyls.

There has been increasing interest in designing ligands that can effectively cap fluorescent semiconductor nanocrystals to make them water soluble, especially to bind to biological molecules or to facilitate easy incorporation into microscopic polymer beads. A family of ligands, which consist of a phosphine oxide binding site, long alkyl chains and a carbon–carbon double bond positioned such that the whole molecule can take part in a polymerisation reaction were used to cap CdSe nanocrystals (see Fig. 1.2). The nanocrystals, thus capped, can be incorporated into microscopic polymer beads by suspension polymerization reactions [24]. Oligomeric phosphines with methacrylate groups have been used to cap CdSe and CdSe–ZnS core–shell nanocrystals and to homogeneously incorporate them into polymer matrices [25]. A polymer ligand consisting of a chain of reactive esters has been successfully used to cap CdSe–ZnS core–shell nanocrystals [26], the pendant reactive groups can be substituted with molecules containing amino-functionalities.

Alivisatos and coworkers have carried out cation exchange reactions on nanocrystals of different shapes and sizes and find that complete and fully reversible

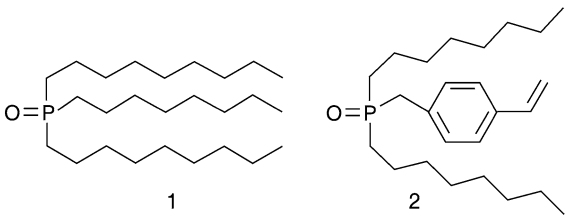

Fig. 1.2 Structure of polymerizable ligands used to cap CdSe nanocrystals.

cation exchange occurs in nanocrystals [27]. Thus, by treating a dispersion of CdSe nanocrystals in toluene with a small volume of methanolic solution of $AgNO_3$, Ag_2Se nanocrystals could be obtained in a few seconds. The rates of the cation exchange reactions on the nanoscale are much faster than in bulk cation exchange processes. This study has also identified a critical size above which the shapes of nanocrystals evolve toward the equilibrium shape with lowest energy during the exchange reaction.

1.2.2 Metal Nanocrystals

Metal nanocrystals have traditionally been prepared by reduction of metal salts. This method has been extremely successful in yielding noble and near-noble metals such as Au, Ag and Pt. However, more reactive metals such as Fe, Cu, Co are not readily obtainable. An organometallic route involving a combination of reduction and thermal decomposition of low or zero valent metal precursors is emerging as an attractive route for the synthesis of metal nanocrystals [28]. This route borrows from previous experience on thermal decomposition to obtain ferro fluids and the use of high boiling alcohols to synthesize metal particles (the polyol method).

Copper nanocrystals have been made by the thermolysis of $[Cu(OCH(Me)CH_2NMe_2)_2]$ in trialkylphosphines or long chain amines [29]. Monodispersed gold nanocrystals with diameters of 9 nm have been prepared by reduction of $HAuCl_4$ in TOPO and octadecylamine [30] (see Fig. 1.3). Palladium nanocrystals in the size range 3.5–7.0 nm have been prepared by thermolysis of a complex with trioctylphosphine [31]. Mesityl complexes of copper, silver and gold have been used as precursors to nanocrystals capped with amines, or triphenyl-

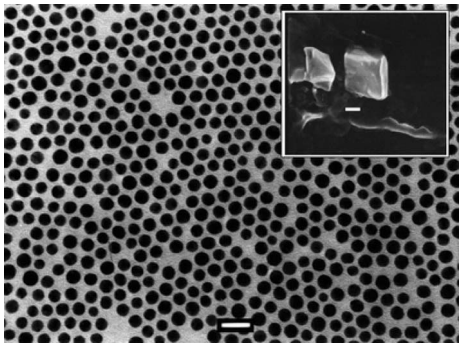

Fig. 1.3 Two-dimensional lattice of octadecylamine/trioctylphosphine oxide-capped gold nanocrystals, bar = 20 nm. Inset: SEM of cubic colloidal crystal prepared from octadecylamine/TOPO-capped gold nanocrystals (190 °C), bar = 80 μm. (reproduced with permission from Ref. [30]).

phosphine oxide [32]. Large nanocrystals of the semimetal bismuth with diameters of 100 nm have been prepared by reduction of bismuth 2-ethylhexanoate in the presence of oleic acid and trialkylphosphine [33]. Lead nanocrystals with diameters of 20 nm have been prepared by thermolysis of tetraethyllead in octanoic acid and trioctylphosphine [34]. Iridium nanocrystals have been prepared by thermolysis of the low-valent organometallic precursor (methylcyclopentadienyl)(1,5-cyclooctadiene)Ir in a mixture of amines [35].

Iron–platinum alloy nanocrystals have attracted a lot of attention, due to their magnetic properties [36]. Iron–platinum nanocrystals with 1:1 ratio of Fe:Pt, exist in two forms. An fcc (face centered cubic) form in which the Fe and Pt atoms are randomly distributed (A1 phase) or an fct (face centered tetragonal) form, in which Fe and Pt layers alternate along the $\langle 001 \rangle$ axis($L1_0$ phase). The latter phase has the highest anisotropic constant among all known magnetic material. Synthesis of homogeneously alloyed Fe–Pt nanocrystals require that Fe and Pt are nucleated at the same time. This process was first accomplished by reducing platinum acetylacetonate with a long chain diol and decomposing $Fe(CO)_5$ in the presence of oleic acid and a long chain amine [37]. There have been several improvements to the original scheme [36]. The as-synthesized nanocrystals are present in the A1 phase and transform into the $L1_0$ phase upon annealing at 560 °C. The transition temperature can be varied by introducing other metal ions. Thus, $[Fe_{49}Pt_{51}]_{88}$ nanocrystals have been made by introduction of silver acetylacetonate in the reaction mixture [38, 39]. The A1 to $L1_0$ transition temperature is lowered to 400 °C by the introduction of Ag ions. Cobalt and copper ions introduced in Fe–Pt nanocrystals by the cobalt acetylacetonate or copper(II)bis(2,2,6,6-tetramethyl-3,5-heptanedionate) resulted in an increase in the A1 to $L1_0$ transition temperature [40, 41]. The successful synthesis of Fe–Pt nanocrystals using a combination of reduction and thermal decomposition to successfully generate homogeneous alloy nanocrystals has sparked a flurry of activity. Thus, CoPt, FePd, $CoPt_3$ have all been obtained [42, 43]. Manganese–platinum alloy nanocrystals have been obtained by using platinum acetylacetonate and $Mn_2(CO)_{10}$ using a combination of reduction and thermal decomposition brought about using 1,2-tetradecanediol in a dioctyl ether, oleic acid/amine medium [44]. Nickel–iron alloy nanocrystals have been obtained using iron pentacarbonyl and $Ni(C_8H_{12})_2$ [45]. Samarium–cobalt alloy nanocrystals have been prepared by thermolysis of cobalt carbonyl and samarium acetylacetonate in dioctyl ether with oleic acid [46]. Similarly, $SmCo_5$ nanocrystals have been prepared using a diol and oleic acid/amine [47].

As can be seen, a wide range of reactive metal and metal alloy nanocrystals have been obtained by thermolysis and/or reduction of organometallic precursors. The key advantage of this method seems be the ability to synthesize alloys of metals, whose reduction potentials are very different.

Alivisatos and coworkers have synthesized hollow nanocrystals by a process analogous to the Kirkendal effect observed in the bulk [48]. In bulk matter, pores are formed in alloying or oxidation reactions due to large differences in the solid-state diffusion rates of the constituents. By reacting Co nanocrystals with S, Se or

oxygen, hollow Co nanocrystals have been obtained. By starting with core–shell nanocrystals of the form Pt–Co and carrying out the process of hole creation, egg-yolk-like nanostructures consisting of a Pt yolk-like core and a Co oxide shell have been obtained.

1.2.3
Nanocrystals of Metal Oxides

Nanocrystals of iron, cobalt, manganese, cobalt and nickel oxides have been synthesized by the thermolysis of the corresponding metal acetylacetonates in hexadecylamine [49]. The nanocrystals could be transferred into the aqueous phase using amine-modified poly(acrylic acid). Nickel oxide nanocrystals obtained by the above method were trigonal (see Fig. 1.4). Manganese oxide nanocrystals of diameter 7 nm have been synthesized by thermal decomposition of manganese acetate in the presence of oleic acid and trioctylamine at high temperature. The MnO nanocrystals so obtained were oxidized to Mn_3O_4 nanocrystals by the use of trimethylamine-*N*-oxide. FeO nanocrystals have also been using the same method [50]. Adopting a similar approach, a range of monodisperse oxide nano-

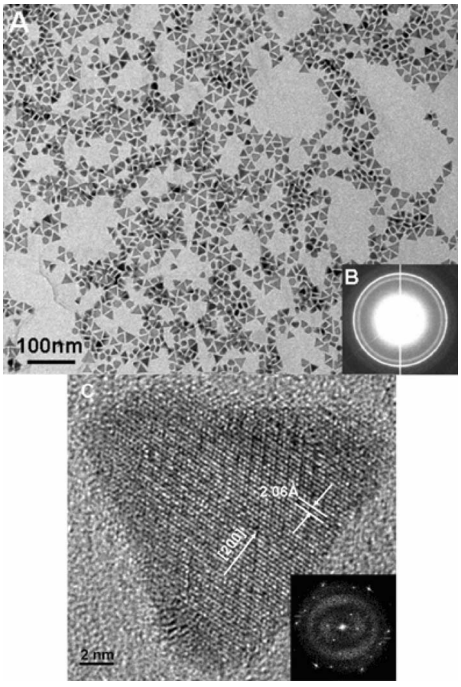

Fig. 1.4 A, TEM image of NiO nanocrystals. B, Electron diffraction pattern acquired from the NiO nanocrystals. C, HRTEM image of NiO nanocrystals, (insert) FFT of the HRTEM.

crystals such as iron oxide, CoO and MnO have been synthesized by decomposition of metal-oleate complexes in different solvents. The oleate complexes were prepared by reacting the corresponding chlorides with Na-oleate [51]. Tetragonal zirconia nanocrystals with diameters of 4 nm have been prepared by a sol–gel process using zirconium(IV) isopropoxide and zirconium(IV) chloride [52].

Biswas and Rao [53] have prepared metallic ReO_3 nanocrystals of different sizes by the solvothermal decomposition of rhenium(VII)oxide–dioxane complex (Re_2O_7–$(C_4H_8O_2)_x$) in toluene. The diameter of the nanocrystals could be varied in the range 8.5–32.5 nm by varying the decomposition conditions. The metallic ReO_3 nanocrystals exhibit a plasmon band similar to Au nanocrystals.

Cobalt oxide nanoparticles with diameters in the 4.5–18 nm range have been prepared by the decomposition of cobalt cupferronate in decalin at 270 °C under solvothermal conditions. Magnetic measurements indicate the presence of ferromagnetic interaction in the small CoO nanoparticles [54]. Cubic and hexagonal CoO nanocrystals have been obtained starting from [Co(acetylacetonate)$_3$] [55]. Nanoparticles of MnO and NiO have been synthesized from cupferronate precursors under solvothermal conditions [56]. Octlyamine capped ZnO nanocrystals with band edge emission have been synthesized using single source precursors zinc cupferronate ($Zn(C_6H_5N_2O_2)_2$, the Zn(II) salt of *N*-nitroso-*N*-phenylhydroxylamine) and a ketoacidoximate ($C_8H_{16}N_2O_8Zn$, diaquabis[2-(methoxyimino) propanoato]zinc(II)) [57].

Yi et al. have embedded magnetic nanocrystals and fluorescent quantum dots in a silica matrix using preformed nanocrystals and carrying out hydrolysis of silicate in a reverse microemulsion [58], building on previously published methods [59, 60]. The nanocomposites thus obtained are water soluble.

Thus, the main areas of research on spherical nanocrystals are directed at the synthesis of unusual materials such as EuS, simplifying synthetic schemes or facilitating the use of nanocrystals by appropriate functionalization.

1.3
Nanocrystals of Different Shapes

1.3.1
Anisotropic Growth of Semiconductor and Oxide Nanocrystals

Nanocrystals of oxides and semiconductors have been grown in different shapes. In a majority of these processes, anisotropic growth is achieved by maintaining a high concentration of the precursors, typically by introducing precursors by continuous or multiple injection. For example, spherical nanocrystals of Cd chalcogenides can be prepared using complexes of Cd and tetradecylphosphonic acid (prepared by reacting CdO with the phosphonic acid) and chalcogen dissolved in trioctylphosphine. By carrying out the same reaction, but maintaining a high concentration of precursors (by multiple injections), nanorods can be produced [61].

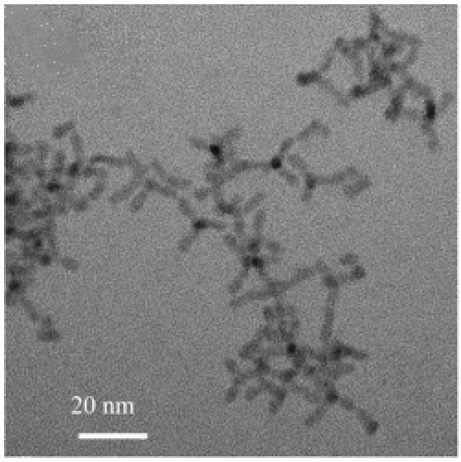

Fig. 1.5 TEM image of CdSe tetrapods (adapted with permission from Ref. [65]).

Cadmium selenide nanocrystals in the form of rods, arrows and branched forms like tetrapods were obtained by introducing the precursor in several steps (see Fig. 1.5) [62–65]. This scheme has been extended to synthesize CdS [66] and CdTe [67] nanocrystals of different shapes. A variety of precursors such as CdO, cadmium naphthenate and single source precursors such as cadmium ethylxanthate [68], cadmium diethyldithiocarbamate [69] have been used to synthesize rods and tetrapods of Cd chalcogenides. Heterostructured tetrapods consisting of CdS, CdSe and CdTe are prepared by alternating the precursors during the injections in the growth step. Thus, arms of CdSe have been grown on CdS nanorods [70]. Tetrapods and rods of MnS and PbS have been obtained by thermal decomposition of the corresponding diethyldithiocarbamate [73, 74]. ZnS nanorods and nanowires have been grown using zinc xanthates [71]. ZnSe nanorods and branched structures have been obtained by decomposing diethylzinc [72]. Narrow nanowires and nanorods of ZnS, CdS, CdSe, ZnSe have been obtained by microwave-assisted decomposition of metal xanthates or mixtures of metal acetates and selenourea [75].

Of particular interest in the synthesis of nanorods is the synthesis of cubic nanorods of sulfides and selenides. Nanorods of CdS have been obtained by reacting Cd-acetate with S in hexadecylamine at high temperatures. High-resolution transmission electron microscopy reveals that the obtained nanorods consist of cubic and hexagonal domains, with the cubic structure predominating [76] (see Fig. 1.6). Cubic CdS nanorods have been obtained solvothermally, starting with $CdCl_2$ and S [77]. Cubic CdSe nanrods have been synthesized by decomposition of the single source precursor $Li_2[Cd_{10}Se_4(SPh_{16})]$ (SPh-phenyl thiolate) [78]. Cubic ZnS nanorods have been obtained by solution-phase aging of spherical ZnS nanocrystals at 60 °C [79].

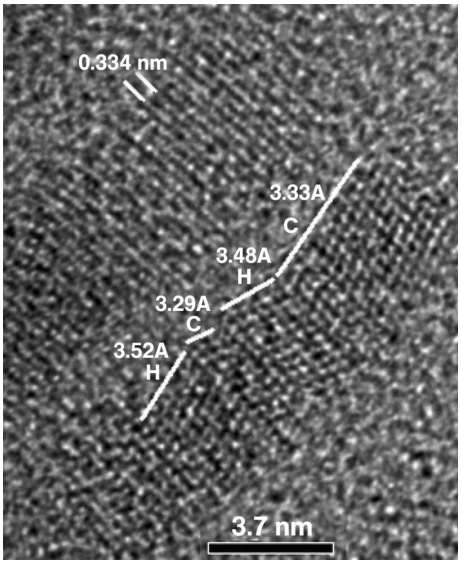

Fig. 1.6 HR-TEM image of a CdS nanorod showing lattice spacing of hexagonal(H) and cubic(C) phases.

A simple one-pot method has been used to prepare CoP nanowires by thermolyis of cobalt(II)acetylacetonate in alkylphosphonic acid in the presence of hexadecylamine and trioctylphosphine oxide [80]. The morphology of the resulting nanowires can be influenced by the ratio of the long chain amine and the phosphine oxide (see Fig. 1.7). Nanorods and nanowires of FeP have been prepared by a similar method [98].

Nanowires, nanotubes, nanowafers and other morphologies of a series of Sb, In and Bi chalcogenides have been obtained by reacting metal acetates with elemental chalcogens in amine [81–83] (see Fig. 1.8). Several of these metal chalcogen phases have been obtained in pure form for the very first time.

Little is understood about the factors determining the growth of anisotropic nanostructures, in particular tetrapods. The tetrapods consist of tetrahedral seeds with cubic structure and arms which are hexagonal. Despite the synthesis of a broad range of semiconductor matter, starting with a wide range of precursors, it is observed that the diameters of the arms of a tetrapod can only be experimentally varied in a narrow size range of 2.0–5.0 nm, leading us to suspect that a fundamental factor underpins the growth of tetrapods. Simple numerical calculations carried out by us suggest that the need to conserve the number of surface atoms plays a crucial role in determining the diameter of the arms of the tetrapods [84]. Branching of tetrahedral seeds is accompanied by a relative gain in the number of surface atoms when the dimensions of the seeds are in the range 2.0–5.0 nm (see Fig. 1.9). Seeds with higher or lower dimensions either suffer an increase in the number of surface atoms or experience marginal rises in the

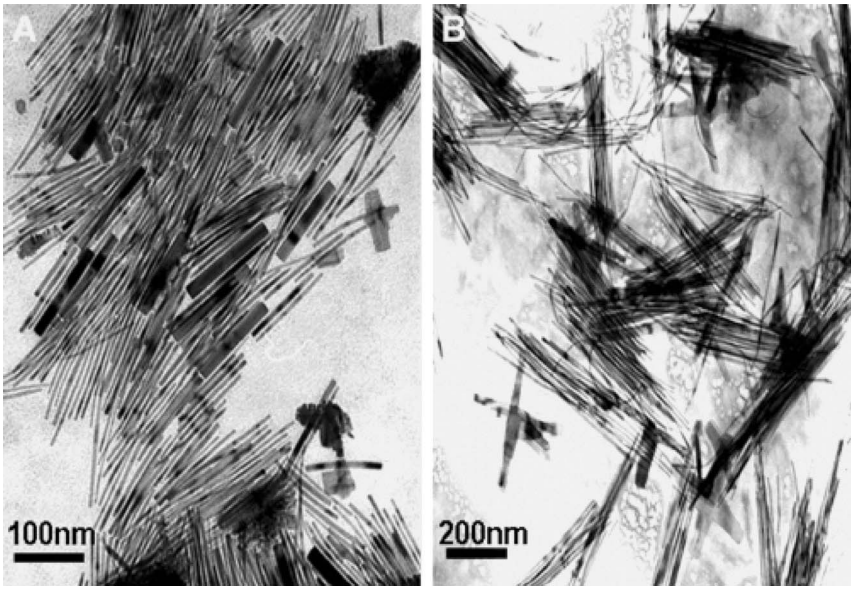

Fig. 1.7 TEM images of CoP nanorods of varying aspect ratios obtained using different ratios of hexadecylamine and triphenylphosphine oxide.

number of surface atoms following branching. The ability to conserve surface atoms lends extra stability to seeds of the right dimensions and plays a key role in determining the dimensions of the tetrapods.

The solution–liquid–solid process is employed for the synthesis of nanorods of more covalent semiconductors. In this method, a metal seed catalyzes the growth of nanorods. Under the growth conditions employed, the seeds form alloys with the nanowire material. The metal seed can either be generated *in situ* or be externally introduced [85]. Building on previous successes, Buhro and coworkers have synthesized GaAs nanowires by decomposition of the single-source precursor $[t\mathrm{Bu_2Ga}\mu\text{-}\mathrm{As(SiMe_3)_2}]_2$ [86]. Ga seeds are generated *in situ* during the decomposition of the precursor. Indium phosphide nanorods have been synthesized by the use of two single source precursors, one to generate the seeds and the other to sustain wire growth. Thus, InP nanorods with diameters controllable in the range 3–9 nm have been obtained using $[t\mathrm{Bu_2InP(SiMe_3)_2}]_2$ and $[\mathrm{Cl_2InP(SiMe_3)_2}]_2$ [87]. Indium arsenide nanorods have been obtained by the use of Au nanocrystals as seeds and $\mathrm{InCl_3}$ and As(trimethylsilane)$_3$ as precursors [88]. The diameters can be varied in the range 4–20 nm by varying the diameters of the seeds. Narrow CdSe nanowires have been obtained using low-melting Bi nanocrystals as seeds [89]. Narrow CdSe and PbSe nanowires have been synthesized using Au/Bi nanocrystals as seeds [90, 91].

Korgel and coworkers have devised a new way to synthesize semiconductor nanowires using supercritical fluids, high temperatures and pressures. By the

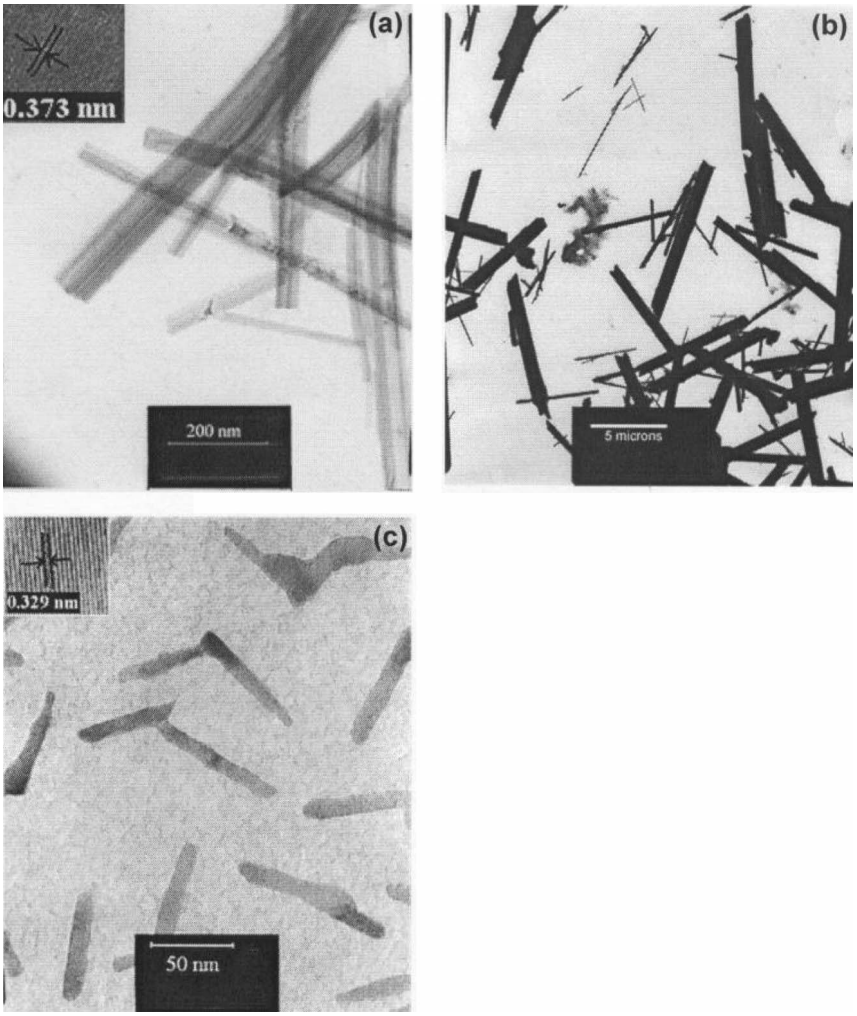

Fig. 1.8 (a) TEM image of InS nanorods (b) TEM image of Sb_2Se_3 nanorods and nanotubes prepared in octylamine (c) TEM image of In_2Te_3 nanorods.

use of this method, seeded growth of nanowires can be achieved in common solvents at high temperatures. Using this process Si [92], Ge [93], GaP [94], GaAs [95] nanowires seeded by either Au or Bi nanocrystals have been successfully obtained (see Fig. 1.10).

Nanorods of ZnO have been obtained by thermolysis of Zn-acetate in a mixture of amines [99]. Iron oxide nanocrystals in cubic, star and other shapes have been obtained by thermolysis of iron carbonyl and acetylacetonates [100]. A number of metal oxide nanocrystals in the form of rods have been obtained by acylhalide

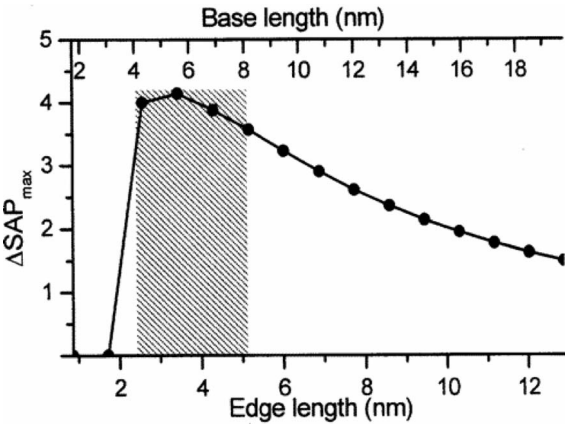

Fig. 1.9 Plot showing changes in the maximum difference in the surface atom percentage (ΔSAP_{max}) between the tetrahedron and the corresponding structures with four hexagonal branches grown from a CdSe seed. The edge length refers to the edge length of the hexagon; the base length pertains to the length of the tetrahedral face from which the branch grows. The size regime for experimentally obtained tetrapods is shaded.

elimination of metal halides in oleylamine [96]. Cubic $BaTiO_3$ nanowires have been synthesized by sol–gel reaction using $BaTi(O_2CCH_3)_6$ [97].

A method related to thermolysis has been used by Korgel and coworkers [101–103] to synthesize nanocrystals in different shapes. In this method, long chain

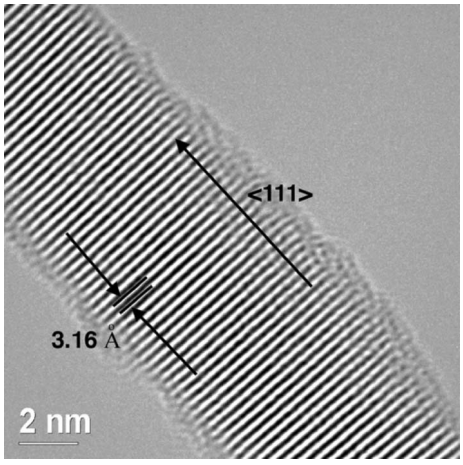

Fig. 1.10 High resolution TEM image of GaP nanowires (reproduced with permission from Ref. [94]).